Cell Reports, Volume *25*

Supplemental Information

PARP Inhibition Elicits STING-Dependent Antitumor Immunity in Brca1-Deficient Ovarian Cancer

Liya Ding, Hye-Jung Kim, Qiwei Wang, Michael Kearns, Tao Jiang, Carolynn E. Ohlson, Ben B. Li, Shaozhen Xie, Joyce F. Liu, Elizabeth H. Stover, Brooke E. Howitt, Roderick T. Bronson, Suzan Lazo, Thomas M. Roberts, Gordon J. Freeman, Panagiotis A. Konstantinopoulos, Ursula A. Matulonis, and Jean J. Zhao

Supplementary Figure S1

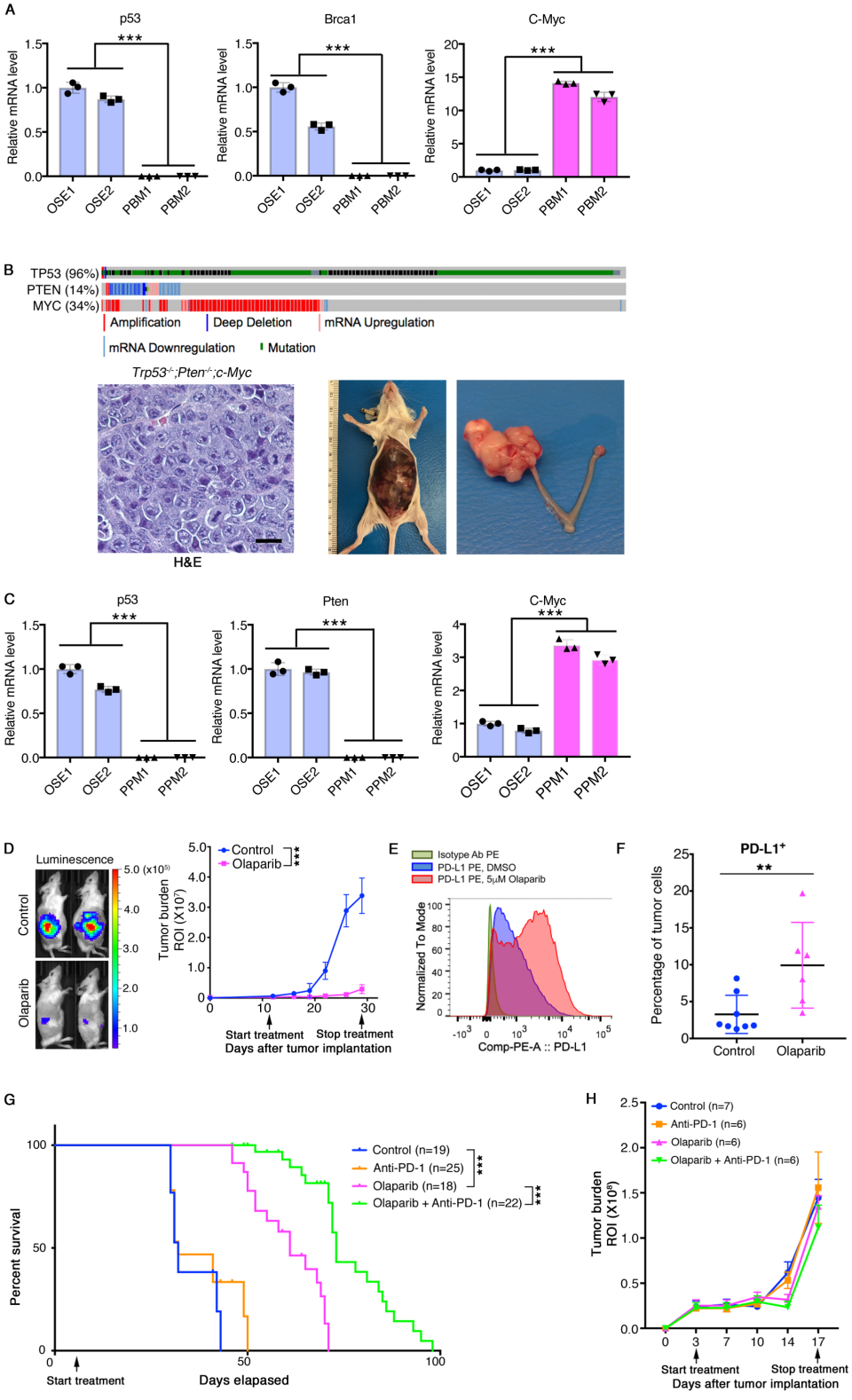

Fig. S1. Characterization of PBM and PPM GEMMs of high-grade serous ovarian cancer (HGSOC). Related to Figure 1. (A) RT-qPCR analysis of the expression levels of *Trp53*, *Brca1* and *c-Myc* of PBM tumor cells and normal ovarian surface epithelial (OSE) cells. (B) Analysis of TCGA database revealed concurrent loss of *Pten* and *Trp53* and amplification of *c-Myc* in clinical samples of HGSOC (upper panel). Representative H&E staining and tumor images of PPM tumor (lower panel). Scale bar, 25 μm. (C) RT-qPCR analysis of the expression levels of *Trp53*, *Pten* and *c-Myc* in PPM tumors. (D) PBM tumor-bearing mice were treated with olaparib or vehicle control for 18 days and tumor burden was measured by bioluminescence (control, n=6; olaparib, n=6). (E) Expression of PD-L1 of cultured PBM cells was analyzed by flow cytometry following olaparib (5μM) treatment for 24 h. (F) Flow cytometry analysis of PD-L1 expression of tumor cells ($CD45^-$) harvested from PBM tumor-bearing mice. (G) Survival curves of PBM tumor bearing mice treated with indicated agents. (H) PPM tumor-bearing mice were treated with indicated agents and tumor burden was measured by bioluminescence. Quantification of the regions of interest (ROI) determined at each imaging time point. Arrow indicates treatment start date. Data are represented as mean ± SD (A, C, F and G) and mean ± SEM (D, H). Each dot represents data obtained from one mouse (C and F). The number of analyzed mice is indicated (G and H). *, $P<0.05$, **, $P<0.01$, ***, $P<0.001$.

Supplementary Figure S2

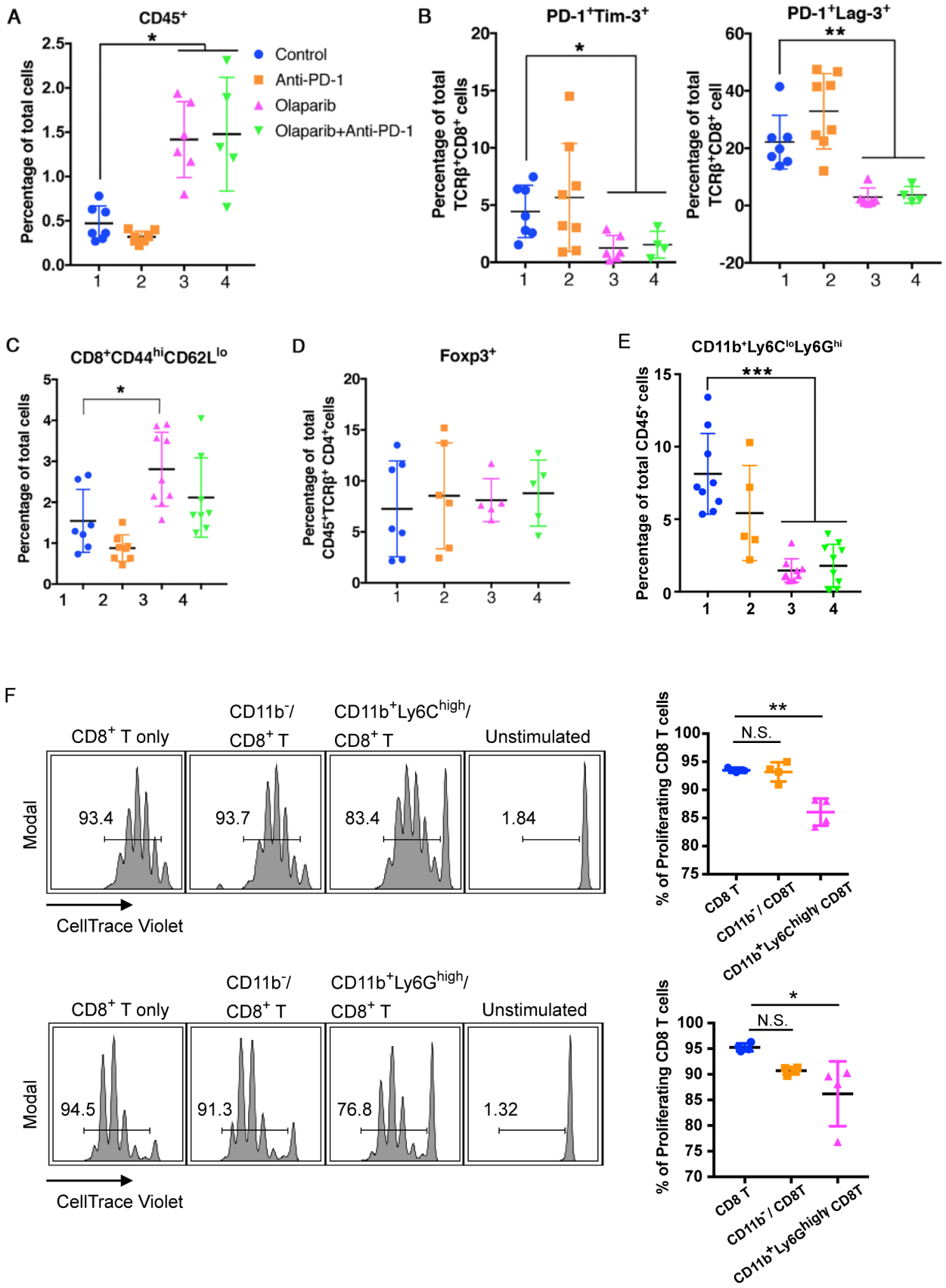

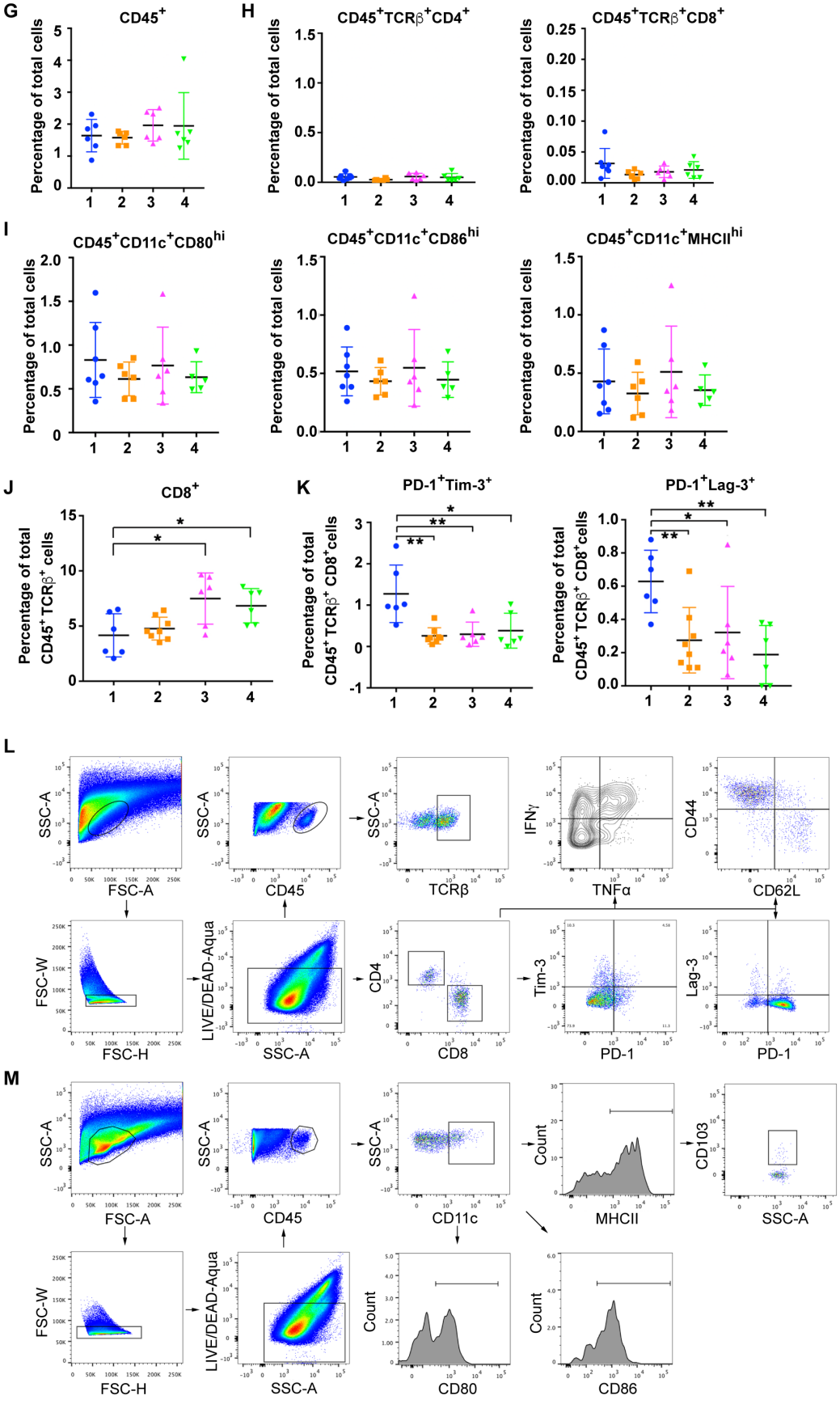
G
CD45+
Percentage of total cells
H
CD45+TCRβ+CD4+
CD45+TCRβ+CD8+
I
CD45+CD11c+CD80hi
CD45+CD11c+CD86hi
CD45+CD11c+MHCIIhi
J
CD8+
Percentage of total CD45+TCRβ+ cells
K
PD-1+Tim-3+
PD-1+Lag-3+
Percentage of total CD45+TCRβ+ CD8+cells
L
SSC-A
FSC-A
CD45
TCRβ
IFNγ
TNFα
CD44
CD62L
FSC-W
FSC-H
LIVE/DEAD-Aqua
CD4
CD8
Tim-3
PD-1
Lag-3
M
CD11c
Count
MHCII
CD103
CD80
CD86

Fig. S2. Olaparib triggers intratumoral and systemic antitumor immune responses in PBM but not in PPM tumor-bearing mice. Related to Figure 2. (A-E) PBM tumor-bearing mice were analyzed by flow cytometry following 21 day treatment for tumor infiltrating leukocytes ($CD45^+$) (A), intratumoral PD-1^+Tim-3^+ or PD-1^+Lag-3^+ $CD8^+$ T cells (B), effector $CD8^+$ T cells ($CD44^{high}CD62L^{low}$) in malignant ascites of peritoneal cavity (C), tumor infiltrating T_{reg} cells ($CD4^+Foxp3^+$) (D), and tumor infiltrating $CD11b^+Ly6C^{low}Ly6G^{high}$ cells (E). (F) $CD8^+$ T cells were co-cultured with $CD11b^+Ly6C^{high}$, $CD11b^+Ly6G^{high}$ cells, or $CD11b^-$ cells sorted from peripheral blood of PBM-tumor bearing mice. CD3/CD28 beads were added to stimulate T cell expansion. $CD8^+$ T cell proliferation was analyzed by flow cytometry using CellTrace™ violet cell proliferation kit. n=4/group. (G-I) Flow cytometric analysis of PPM tumor infiltrating leukocytes (G), T cells (H) and activation cell surface markers of dendritic cells (I) following indicated treatment. (J, K) Flow cytometric analysis of splenic immune cell populations in PBM tumor-bearing mice for $CD8^+$ T cells (J) and exhausted $CD8^+$ T cells (K). (L, M) Gating strategies of T cell (L) and dendritic cells (M). Data are represented as mean ± SD. Each dot represents data obtained from one mouse. *, $P<0.05$, **, $P<0.01$, ***, $P<0.001$. N.S., not significant.

Supplementary Figure S3

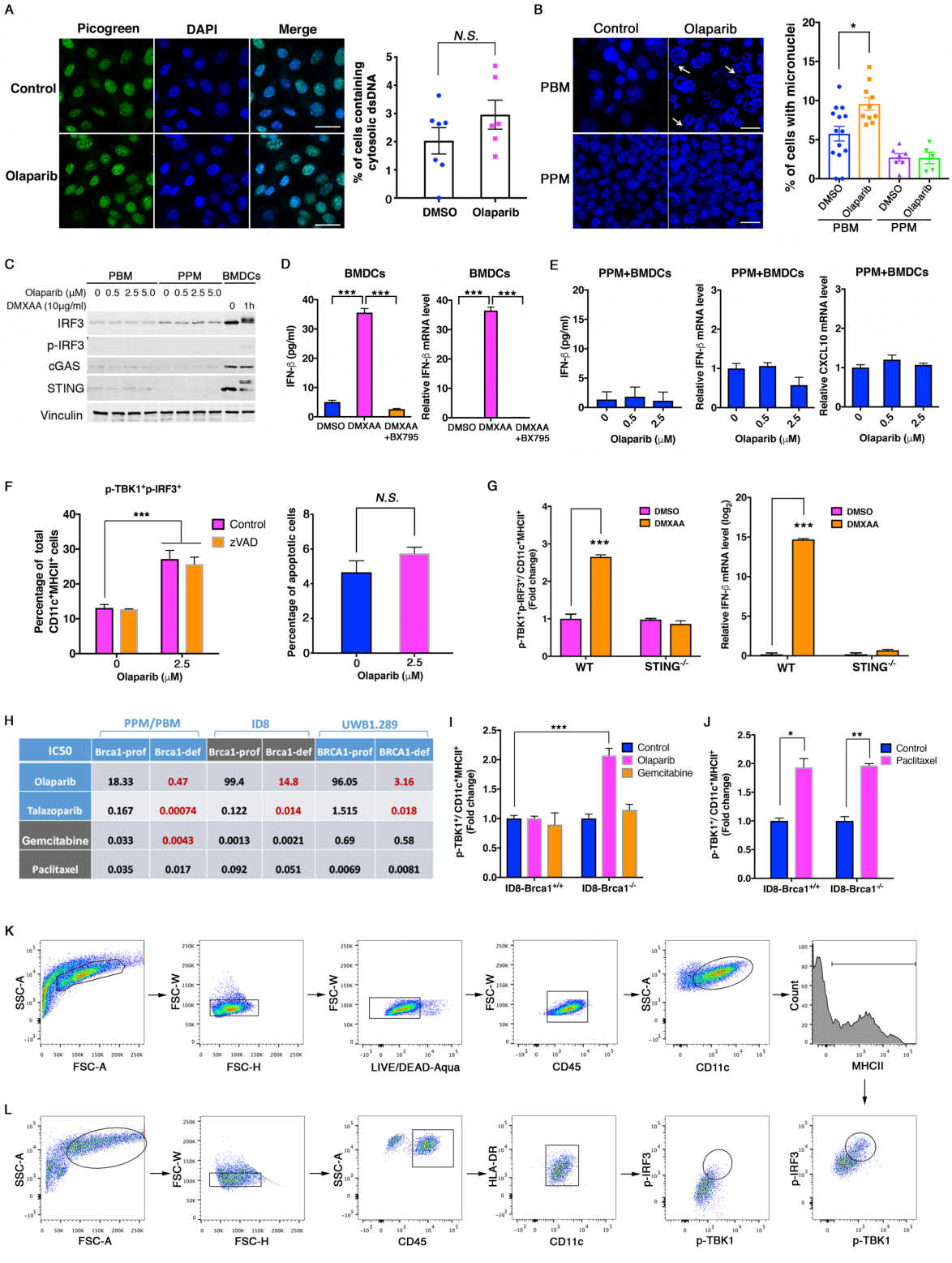

IC50	PPM/PBM		ID8		UWB1.289	
	Brca1-prof	Brca1-def	Brca1-prof	Brca1-def	BRCA1-prof	BRCA1-def
Olaparib	18.33	0.47	99.4	14.8	96.05	3.16
Talazoparib	0.167	0.00074	0.122	0.014	1.515	0.018
Gemcitabine	0.033	0.0043	0.0013	0.0021	0.69	0.58
Paclitaxel	0.035	0.017	0.092	0.051	0.0069	0.0081

Fig. S3. Activation of the STING pathway in dendritic cells co-cultured with olaparib treated *Brca1*-deficient tumor cells. Related to Figure 3. (A) Representative staining of cytosolic double strand DNA (dsDNA) by PicoGreen in PPM tumor cells treated with DMSO or 2.5 μM olaparib for 24 h, scale bar, 25 μm. (B) Representative DAPI staining of primary nucleus and micronucleus (indicated by arrows). Percentage of cells with micronucleus is calculated (right). (C) Western blot analysis of cGAS-STING and its signaling molecules in olaparib-treated PBM and PPM tumors cells. DMXAA, a murine STING agonist, treated bone marrow derived dendritic cells (BMDCs) served as a positive control. (D) Analysis of IFN-β level in BMDCs culture media and cells were analyzed by ELISA (left) and RT-qPCR (right), respectively. To modulate STING signaling pathway, DMXAA (5μg/ml, 2 h) and a STING inhibitor BX795 (2μM, 2h) were employed. (E) BMDCs were co-cultured with pretreated PPM cells. IFN-β in the co-culture media and IFN-β and CXCL10 mRNA in BMDCs were analyzed by ELISA and RT-qPCR, respectively. (F) Flow cytometric analysis of STING pathway activation (indicated by phosphorylated TBK1 and IRF3) in BMDCs from BMDC/PBM co-culture. Prior to co-culture with BMDCs, PBM cells pre-treated with olaparib (2.5μM) in the presence or absence of an apoptosis inhibitor zVAD (10μM) for 24 h. (G) Flow cytometric analysis of phosphorylated TBK1 and IRF3 (left) and RT-qPCR analysis of IFN-β (right) in wild type (WT) and $STING^{-/-}$ BMDCs stimulated with DMXAA (5μg/ml) for 2 hours. (H) IC50 values for PARP inhibitors and other cytotoxic agents in BRCA1-proficient and -deficient tumor cells. (I, J) Flow cytometric analysis of phosphorylated TBK1 and IRF3 in BMDCs co-cultured with WT or *Brca1*-null ID8 cells with indicated treatments. (K, L) Gating strategies of phosphorylated TBK1 and IRF3 in $CD11c^{+}$dendritic cells in murine BMDCs (J) and human DCs (K). Data are represented as mean ± SD; n=3 unless indicated otherwise; *, $P<0.05$, **, $P<0.01$, ***, $P<0.001$.

Supplementary Figure S4

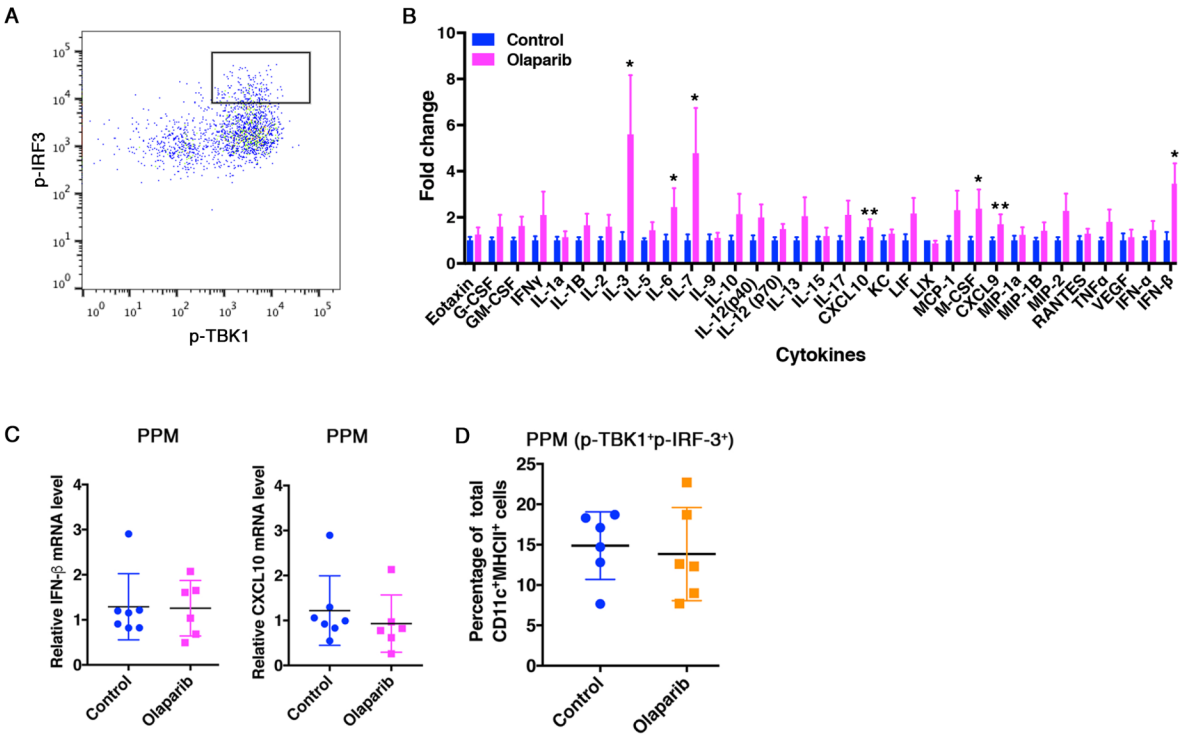

Fig. S4. STING pathway activation is required for the therapeutic efficacy of PARP inhibitors in *Brca1*-deficient tumors. Related to Figure 4. (A) Gating strategies of phosphorylated TBK1 and IRF3 of CD11c^{+} dendritic cells in PBM and PPM tumors. (B) Cytokine array of sera collected from PBM tumor-bearing mice treated with vehicle or olaparib for 2 days. (Control, n=9; Olaparib, n=7). (C) RT-qPCR analysis of IFN-β and CXCL10 in DCs isolated from PPM tumors of tumor-bearing mice treated with vehicle control or olaparib-treated. (Control, n=7; Olaparib, n=6). (D) Flow cytometric analysis of phosphorylated TBK1 and IRF3 in PPM tumor infiltrating DCs following indicated treatment. Data are represented as mean ± SD. Each dot represents data obtained from one mouse (C and D). *, P<0.05; **, P<0.01.